This article was downloaded by: [Renmin University of China]
On: 13 October 2013, At: 10:30
Publisher: Taylor & Francis
Informa Ltd Registered in England and Wales Registered Number: 1072954 Registered office: Mortimer House, 37-41 Mortimer Street, London W1T 3JH, UK

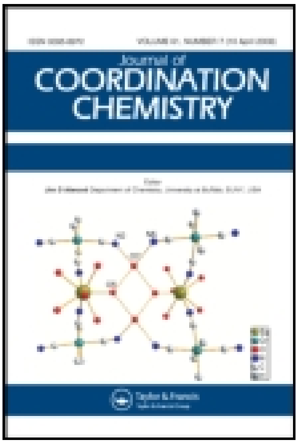

Journal of Coordination Chemistry
Publication details, including instructions for authors and subscription information:
http://www.tandfonline.com/loi/gcoo20

Synthesis, molecular and electronic structures of half-sandwich ruthenium(II) complexes with 2,2′-bis(4,5-dimethylimidazolyl) and 4,5-diphenylimidazole ligands

J.G. Małecki [a]

[a] Department of Crystallography , Institute of Chemistry, University of Silesia , 9th Szkolna St., 40-006 Katowice, Poland

Published online: 18 Jan 2011.

To cite this article: J.G. Małecki (2011) Synthesis, molecular and electronic structures of half-sandwich ruthenium(II) complexes with 2,2′-bis(4,5-dimethylimidazolyl) and 4,5-diphenylimidazole ligands, Journal of Coordination Chemistry, 64:3, 390-399, DOI: 10.1080/00958972.2010.550614

To link to this article: http://dx.doi.org/10.1080/00958972.2010.550614

PLEASE SCROLL DOWN FOR ARTICLE

Taylor & Francis makes every effort to ensure the accuracy of all the information (the "Content") contained in the publications on our platform. However, Taylor & Francis, our agents, and our licensors make no representations or warranties whatsoever as to the accuracy, completeness, or suitability for any purpose of the Content. Any opinions and views expressed in this publication are the opinions and views of the authors, and are not the views of or endorsed by Taylor & Francis. The accuracy of the Content should not be relied upon and should be independently verified with primary sources of information. Taylor and Francis shall not be liable for any losses, actions, claims, proceedings, demands, costs, expenses, damages, and other liabilities whatsoever or howsoever caused arising directly or indirectly in connection with, in relation to or arising out of the use of the Content.

This article may be used for research, teaching, and private study purposes. Any substantial or systematic reproduction, redistribution, reselling, loan, sub-licensing, systematic supply, or distribution in any form to anyone is expressly forbidden. Terms &

Conditions of access and use can be found at http://www.tandfonline.com/page/terms-and-conditions

Downloaded by [Renmin University of China] at 10:30 13 October 2013

Journal of Coordination Chemistry
Vol. 64, No. 3, 10 February 2011, 390–399

Taylor & Francis
Taylor & Francis Group

Synthesis, molecular and electronic structures of half-sandwich ruthenium(II) complexes with 2,2′-bis(4,5-dimethylimidazolyl) and 4,5-diphenylimidazole ligands

J.G. MAŁECKI*

Department of Crystallography, Institute of Chemistry, University of Silesia,
9th Szkolna St., 40-006 Katowice, Poland

(*Received 8 July 2010; in final form 8 November 2010*)

In this study, [(C_6H_6)RuCl(DMDIm)]Cl and [(C_6H_6)RuCl$_2$(4,5-Ph$_2$Im)] have been prepared and studied by infrared, NMR, UV-Vis spectroscopy, and X-ray crystallography. The complexes were prepared in reactions of [(C_6H_6)RuCl$_2$]$_2$ with 2,2′-bis(4,5-dimethylimidazolyl) and 4,5-diphenylimidazole in methanol. The electronic structure and UV-Vis spectrum of the obtained compounds have been calculated using the TD-DFT method.

Keywords: Ruthenium benzene complexes; 2,2′-Bis(4,5-dimethylimidazolyl); 4,5-Diphenylimidazole; X-ray structure; UV-Vis; DFT; TD-DFT

Downloaded by [Renmin University of China] at 10:30 13 October 2013

1. Introduction

The coordination chemistry of ruthenium complexes containing N-heterocyclic derivatives is well-studied because of very rich redox chemistry and photophysics. Even small changes in coordination environment around ruthenium play a key role in altering the redox properties of its complexes, and thus complexation of ruthenium by various ligands has been widely studied. The η^6-arene ruthenium complexes play a vital role in organometallic chemistry [1] with arene ruthenium halide compounds key starting materials for the formation of a wide range of neutral and cationic ligand derivatives [2]. Half-sandwich arene ruthenium complexes serve as excellent catalyst precursors for hydrogenation and for ring-opening metathesis polymerization. Some studies of arene ruthenium complexes show that they can inhibit cancer cell growth [3].

The compounds in this manuscript combine the benefits of ruthenium coordination compounds and complexes containing 2,2′-bis(4,5-dimethylimidazolyl) or 4,5-diphenylimidazole. This article presents the synthesis, crystal, molecular, and electronic structures and the spectroscopic characterization of two new half-sandwich ruthenium(II) complexes.

---

*Email: gmalecki@us.edu.pl

Journal of Coordination Chemistry
ISSN 0095-8972 print/ISSN 1029-0389 online © 2011 Taylor & Francis
DOI: 10.1080/00958972.2010.550614

Downloaded by [Renmin University of China] at 10:30 13 October 2013

2. Experimental

The starting material $[(C_6H_6)RuCl_2]_2$ was synthesized according to the literature procedure [4]. All other reagents were commercially available and used without purification.

2.1. *Synthesis of the complexes*

A mixture of $[(C_6H_6)RuCl_2]_2$ (0.25 g; $5 \cdot 10^{-4}$ mol) and 2,2′-bis(4,5-dimethylimidazolyl) (0.13 g; $\sim 7 \cdot 10^{-4}$ mol) or 4,5-diphenylimidazole (0.15 g; $\sim 0.7 \cdot 10^{-4}$ mol) in methanol (50 cm^{-3}) was refluxed for 3 h, cooled, and filtered. Crystals suitable for X-ray crystal analysis were obtained by slow evaporation of the reaction mixture.

1: $[(C_6H_6)RuCl(DMDIm)]Cl \cdot CH_3OH$ – Yield 80%. Infrared (IR) (KBr): 3386 (ν_{NH}), 3075 (ν_{CH}), 2948 (ν_{CH}), 1764 (ν_{ring}), 1595 (ν_{CN}), 1516 ($\nu_{C=C}$), 1429 ($\nu_{ring} + \nu_{CH}$), 1376 (δ_{CH}), 1210 (δ_{CH}), 854 (γ_{CH}), 582 ($\nu_{Ru\text{–}N}$). UV-Vis (methanol, λ (nm) ($\log \varepsilon$)): 449.6 (2.19), 314.5 (3.84), 210.1 (4.08). ^{1}H-NMR: ($CDCl_3$, ppm) 13.466 (s, NH), 5.889 (s, C_6H_6), 3.503 (CH_3OH), 2.440 (s, CH_3). Anal. Calcd for: C, 43.23%; H, 5.12%; Cl, 15.01%; N, 11.86%; O, 3.39%; Ru, 21.40%. Found: C, 42.43%; H, 5.21%; N, 11.95%.

2: $[(C_6H_6)RuCl_2(4,5\text{-}Ph_2Im)] \cdot CH_3OH$ – Yield 86%. IR (KBr): 3402 (ν_{NH}), 3154 (ν_{CH}), 3074 (ν_{CH}), 3055 (ν_{CH}), 1603 (ν_{CN}), 1496 ($\nu_{C=C}$), 1434 ($\nu_{ring} + \nu_{CH}$), 1335 (δ_{CH}), 918 (γ_{CH}), 537 ($\nu_{Ru\text{–}N}$). UV-Vis (acetonitrile, λ [nm] ($\log \varepsilon$)): 412.6 (3.70), 283.2 (4.86), 228.6 (5.07), 210.8 (4.98) nm. ^{1}H-NMR: ($CDCl_3$, ppm) 11.220 (s, NH), 8.399 (d, H2), 7.481–7.261 (m, PhH), 5.193 (s, C_6H_6), 3.508 (CH_3OH). Anal. Calcd for: C, 52.28%; H, 4.99%; Cl, 14.03%; N, 5.54%; O, 3.17%; Ru, 20.00%. Found: C, 52.23%; H, 5.10%; N, 5.55%.

2.2. *Physical measurements*

IR spectra were recorded on a Nicolet Magna 560 spectrophotometer from 4000to 400 cm^{-1} as KBr pellets. Electronic spectra were measured on a Lab Alliance UV-Vis 8500 spectrophotometer from 600 to 180 nm in methanol. Elemental analyses (C, H, and N) were performed on a Perkin-Elmer CHN-2400 analyzer. ^{1}H-NMR spectra were obtained at room temperature in $CDCl_3$ using a Bruker 400 spectrometer.

2.3. *DFT calculations*

The calculations were carried out using Gaussian 09 [5]. The DFT/B3LYP [6] method was used for geometry optimization and electronic structure determination, and electronic spectra were calculated by the TD-DFT [7] method. The calculations were performed using the DZVP basis set [8] with *f* functions with exponents 1.94722036 and 0.748930908 on ruthenium, and polarization functions for all other atoms: 6–31 g(2d, p) – chlorine, 6–31 g** – carbon, nitrogen, and 6–31 g(d, p) – hydrogen. The PCM solvent model was used in the Gaussian calculations with acetonitrile as the solvent. GaussSum 2.2 [9] was used to calculate group contributions to the molecular orbitals and to prepare the partial density of states (DOS) and overlap population density of states (OPDOS) spectra. The contribution of a group to a molecular orbital was calculated

Downloaded by [Renmin University of China] at 10:30 13 October 2013

Table 1. Crystal data and structure refinement details of $[(C_6H_6)RuCl(DMDIm)]Cl \cdot CH_3OH$ (**1**) and $[(C_6H_6)RuCl_2(4,5\text{-}Ph_2Im)]$ (**2**).

	1	**2**
Empirical formula	$C_{17}H_{24}Cl_2N_4ORu$	$C_{22}H_{22}Cl_2N_2ORu$
Formula weight	472.37	502.39
Temperature (K)	295.0(2)	295.0(2)
Crystal system	Monoclinic	Monoclinic
Space group	$P2(1)/c$	$P2(1)/c$
Unit cell dimensions (Å, °)		
a	10.8379(5)	15.1668(2)
b	12.5642(5)	6.78120(9)
c	14.6000(5)	20.8498(3)
β	90.989(3)	95.4838(14)
Volume (Å^3), Z	1987.77(13), 4	2134.57(5), 4
Calculated density ($Mg\,m^{-3}$)	1.578	1.563
Absorption coefficient (mm^{-1})	1.070	1.000
$F(0\,0\,0)$	960	1016
Crystal size (mm^3)	$0.195 \times 0.193 \times 0.178$	$0.255 \times 0.161 \times 0.027$
θ range for data collection (°)	3.39–25.05	3.39–25.24
Limiting indices	$-12 \le h \le 12$; $-14 \le k \le 14$; $-17 \le l \le 17$	$-18 \le h \le 18$; $-8 \le k \le 8$; $-24 \le l \le 24$
Reflections collected	12,156	20,814
Independent reflections	3436 [R(int) = 0.0316]	3763 [R(int) = 0.0278]
Data/restraints/parameters	3436/0/239	3763/0/258
Goodness-of-fit on F^2	1.169	1.007
Final R indices [$I > 2\sigma(I)$]	$R_1 = 0.0372$, $wR_2 = 0.0896$	$R_1 = 0.0201$, $wR_2 = 0.0487$
R indices (all data)	$R_1 = 0.0533$, $wR_2 = 0.0947$	$R_1 = 0.0278$, $wR_2 = 0.0499$
Largest difference peak and hole (e Å^{-3})	0.823 and −0.618	0.254 and −0.230

using Mulliken population analysis. The PDOS and OPDOS spectra were created by convoluting the molecular orbital information with Gaussian curves of unit height and FWHM of 0.3 eV.

2.4. *Crystal structure determination and refinement*

Red crystals of $[(C_6H_6)RuCl(2,2'\text{-}(4,5\text{-}(CH_3)_2Im)_2)]Cl \cdot CH_3OH$ and $[(C_6H_6)RuCl_2(4,5\text{-}Ph_2Im)] \cdot CH_3OH$ were mounted in turn on an Xcalibur, Atlas, Gemini ultra Oxford Diffraction automatic diffractometer equipped with a CCD detector and used for data collection. X-ray intensity data were collected with graphite monochromated Mo-Kα radiation ($\lambda = 0.71073$ Å) at 295.0(2) K, with ω scan mode. Ewald sphere reflections were collected up to $2\theta = 58.48°$. Unit cell parameters were determined from least-squares refinement of the setting angles of 6729 for **1**, and 20,814 for **2**, strongest reflections. Details concerning crystal data and refinement are gathered in table 1. During data reduction, the decay correction coefficient was taken into account. Lorentz, polarization, and numerical absorption corrections were applied. The structures were solved by the Patterson method. All non-hydrogen atoms were refined anisotropically using full-matrix, least-squares on F^2. All hydrogens were found from difference Fourier synthesis after four cycles of anisotropic refinement, and refined as "riding" on the adjacent atom with individual isotropic temperature factor equal to 1.2 times the value of equivalent temperature factor of the parent atom, with geometry idealization after each cycle. Olex2 [10] program was used for all calculations. Atomic scattering factors were those incorporated in the computer programs.

3. Results and discussion

The half-sandwich complexes were obtained by the reaction of $[(C_6H_6)RuCl_2]_2$ with 2,2′-bis(4,5-dimethylimidazolyl) (DMDIm) and 4,5-diphenylimidazole (4,5-Ph_2Im) in methanol. The elemental analyses of the complexes are in good agreement with their formulations. In the IR spectrum of **1**, the ring C=C and C=N stretching mode bands of 2,2′-bis(4,5-dimethylimidazolyl) are present at $1720\,cm^{-1}$, $1636\,cm^{-1}$ and for **2**, 4,5-diphenylimidazole C=C and C=N stretches are at $1603\,cm^{-1}$. The ν_{NH} bands are at $3386\,cm^{-1}$ for **1** and $3402\,cm^{-1}$ for **2**. The stretching modes of the aryl C–H are observed at $3075\,cm^{-1}$, and 3154, 3074, $3055\,cm^{-1}$ for **1** and **2**, respectively. Methyl stretching in the 2,2′-bis(4,5-dimethylimidazolyl) has a maximum at $2948\,cm^{-1}$ and the bend mode of CH_3 at $1210\,cm^{-1}$. The stretching frequencies of the Ru–N bond are at $582\,cm^{-1}$ in **1** and $537\,cm^{-1}$ in **2**. In ^{1}H-NMR spectra of the complexes, the protons of η^6–C_6H_6 appear as a singlet at 5.887 ppm and 5.193 ppm, the NH protons of 2,2′-bis(4,5-dimethylimidazolyl) at 13.466 ppm, and the ones of 4,5-diphenylimidazole at 11.220 ppm for **1** and **2**, respectively.

3.1. *Crystal structures*

Both complexes crystallize in the monoclinic space group $P2(1)/c$ with molecular structures shown in figure 1. Selected bond lengths and angles are listed in table 2. The complexes adopt a distorted piano-stool geometry with ruthenium π-bonded to the benzene ring with an average Ru–C distance of 2.173(5) Å in **1** and 2.1565(2) (range 2.149(2)–2.169(2) Å) in **2**; the distances between ruthenium and the centroid of the benzene ring are 1.671 Å and 1.653 Å for **1** and **2**, respectively. The ruthenium is also directly coordinated to nitrogens of N-heterocyclic ligands with normal distances. The Ru–Cl bond lengths are also normal and comparable to other ruthenium(II) half-sandwich complexes. The angles between nitrogen and chloride ligands in **1** and **2** are close to those observed in ruthenium arene compounds [11]. In the structures of both complexes, inter- and intra-molecular weak hydrogen bonds [12] exist and are collected in table 3.

3.2. *Geometry and electronic structure*

To provide insight into the electronic structures and bonding properties of **1** and **2**, DFT calculations were carried out. Before calculations of electronic structures of the complexes, their geometries were optimized in singlet states using the DFT method with the B3LYP functional. From the data collected in table 2, one may see that the majority of differences between the experimental and calculated geometries are found in the benzene ligand. The largest differences were found for ruthenium–benzene carbon distances. The calculated Ru–benzene centroid distances are 1.747 Å for **1** and 1.719 Å for **2**. For the optimized angles, the maximum differences from the experimental values

Downloaded by [Renmin University of China] at 10:30 13 October 2013

Downloaded by [Renmin University of China] at 10:30 13 October 2013

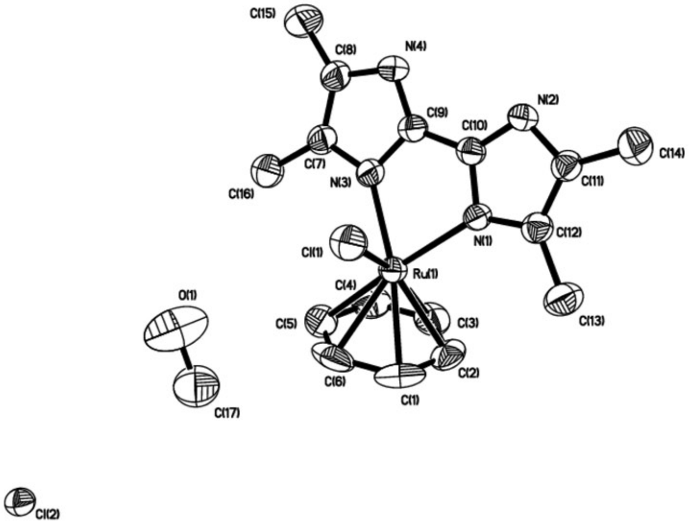

1

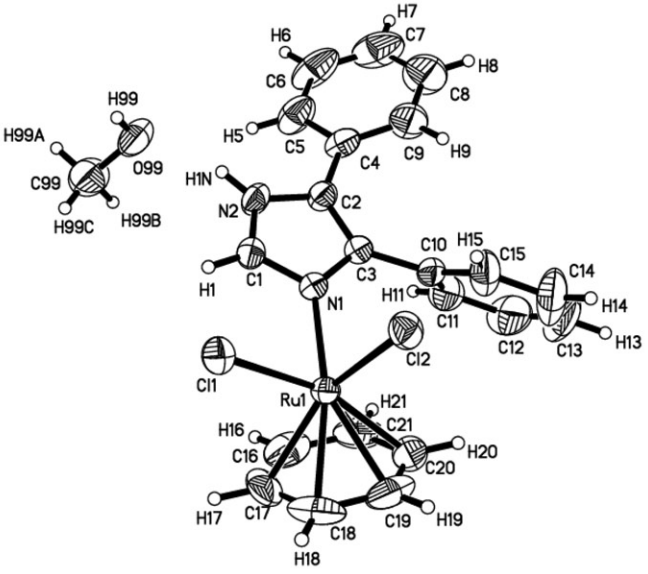

2

Figure 1. ORTEP drawings of $[(C_6H_6)RuCl(DMDIm)]Cl \cdot CH_3OH$ and $[(C_6H_6)RuCl_2(4,5\text{-}Ph_2Im)]$ with 50% probability displacement ellipsoids. Hydrogens are omitted for clarity.

are in Cl(1)–Ru(1)–C(5) and N(1)–Ru(1)–Cl(1) (8.17° for **1**) and in N(1)–Ru(1)–Cl(1) (3.17° for **2**).

In the frontier region, neighboring orbitals may show quasi-degeneracy of the energy levels. In such cases, consideration of only the HOMO and LUMO may not yield

Downloaded by [Renmin University of China] at 10:30 13 October 2013

Table 2. Selected bond lengths (Å) and angles (°) for **1** and **2** with the optimized geometry values.

1			**2**		
	Experimental	Calculated		Experimental	Calculated
Ru(1)–N(1)	2.114(3)	2.1556	Ru(1)–N(1)	2.1519(15)	2.2079
Ru(1)–N(3)	2.119(3)	2.1566	Ru(1)–Cl(1)	2.4150(5)	2.4279
Ru(1)–Cl(1)	2.3934(10)	2.3994	Ru(1)–Cl(2)	2.4220(5)	2.4552
Ru(1)–C(1)	2.169(5)	2.2499	Ru(1)–C(16)	2.160(2)	2.2568
Ru(1)–C(2)	2.177(4)	2.2400	Ru(1)–C(17)	2.152(2)	2.2197
Ru(1)–C(3)	2.185(5)	2.2873	Ru(1)–C(18)	2.169(2)	2.2152
Ru(1)–C(4)	2.163(5)	2.2407	Ru(1)–C(19)	2.155(2)	2.2105
Ru(1)–C(5)	2.184(5)	2.2506	Ru(1)–C(20)	2.154(2)	2.2476
Ru(1)–C(6)	2.161(5)	2.2386	Ru(1)–C(21)	2.149(2)	2.2332
N(1)–Ru(1)–N(3)	77.24(13)	76.45	Cl(1)–Ru(1)–Cl(2)	84.78(19)	88.68
N(1)–Ru(1)–Cl(1)	82.27(9)	84.29	N(1)–Ru(1)–Cl(1)	87.15(5)	88.03
N(3)–Ru(1)–Cl(1)	85.65(9)	84.26	N(1)–Ru(1)–Cl(2)	88.87(4)	84.72
N(1)–Ru(1)–C(1)	113.50(19)	108.33	N(1)–Ru(1)–C(19)	148.61(10)	148.73
N(1)–Ru(1)–C(3)	101.98(16)	107.15	N(1)–Ru(1)–C(21)	89.66(8)	93.16
N(1)–Ru(1)–C(5)	167.61(18)	172.50	N(1)–Ru(1)–C(17)	125.22(11)	128.39
N(3)–Ru(1)–C(1)	169.19(19)	172.46	Cl(1)–Ru(1)–C(19)	123.77(9)	122.32
N(3)–Ru(1)–C(3)	110.95(17)	107.13	Cl(1)–Ru(1)–C(21)	147.12(9)	144.73
N(3)–Ru(1)–C(5)	101.30(18)	108.27	Cl(1)–Ru(1)–C(17)	87.39(7)	85.16
Cl(1)–Ru(1)–C(1)	96.84(15)	101.85	Cl(2)–Ru(1)–C(19)	88.84(7)	88.39
Cl(1)–Ru(1)–C(3)	163.36(15)	165.26	Cl(2)–Ru(1)–C(21)	127.89(8)	126.55
Cl(1)–Ru(1)–C(5)	109.99(16)	101.82	Cl(2)–Ru(1)–C(17)	144.57(10)	145.92
C(1)–Ru(1)–C(3)	66.6(2)	66.13	C(21)–Ru(1)–C(17)	68.04(11)	66.68
C(1)–Ru(1)–C(5)	67.9(2)	66.38	C(19)–Ru(1)–C(21)	67.54(11)	66.94
C(3)–Ru(1)–C(5)	66.81(19)	66.12	C(19)–Ru(1)–C(17)	67.31(11)	67.28

Table 3. Hydrogen bonds for **1** and **2** (Å and °).

D–H···A	*d*(D–H)	*d*(H···A)	*d*(D···A)	∠(DHA)
1				
N(2)–H(1)···Cl(2) #1	0.86	2.48	3.262(4)	151.0
N(4)–H(12)···Cl(2) #1	0.83(4)	2.35(5)	3.126(4)	158.0(4)
O(1)–H(14)···Cl(2) #2	1.04(11)	2.11(11)	3.145(6)	171.0(9)
C(1)–H(2)···Cl(2) #3	0.93	2.82	3.674(6)	153.2
C(3)–H(4)···Cl(1) #4	0.93	2.82	3.481(5)	128.6
C(14)–H(9B)···Cl(1) #5	0.96	2.82	3.652(5)	147.8
2				
C(1)–H(1)···Cl(1)	0.93	2.58	3.128(2)	117.7
C(15)–H(15)···Cl(2)	0.93	2.70	3.368(3)	129.3

Symmetry transformations used to generate equivalent atoms: #1: $-1+x$, $1+y$, z; #2: $1-x$, $1/2+y$, $1/2-z$; #3: x, $1+y$, z; #4: x, $3/2-y$, $-1/2+z$; #5: $-x$, $1/2+y$, $1/2-z$.

a realistic description of the frontier orbitals. For this reason, partial DOS and OPDOS in terms of Mulliken population analysis were calculated using the GaussSum program. They provide a pictorial representation of MO compositions and their contributions to chemical bonding. The DOS and OPDOS diagrams are shown in figure 2. The DOS plot mainly presents the composition of the fragment orbitals contributing to the molecular orbitals. The OPDOS allows us to ascertain the bonding, non-bonding,

Downloaded by [Renmin University of China] at 10:30 13 October 2013

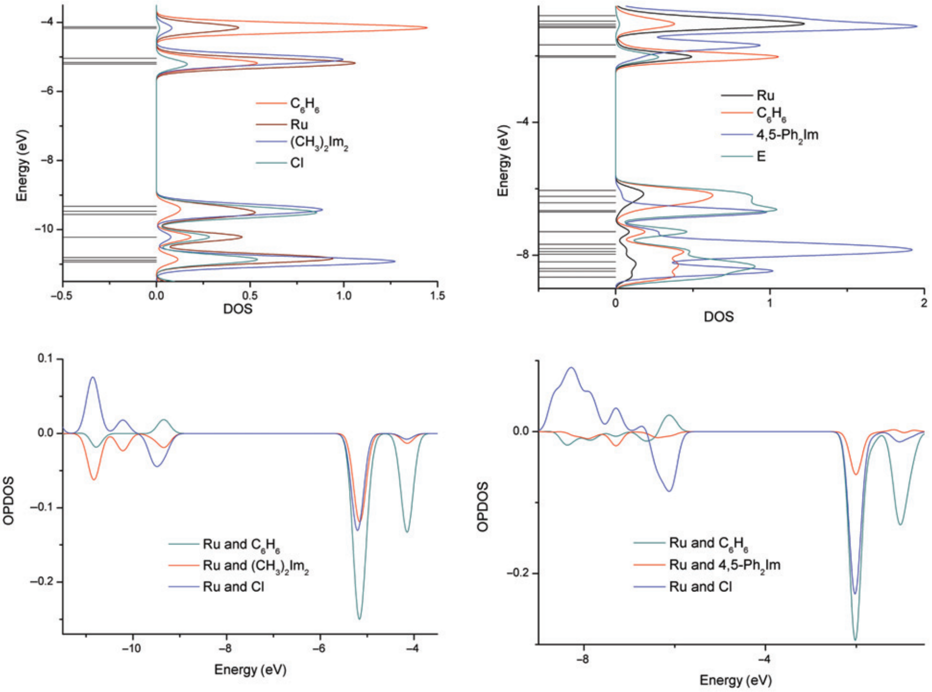

Figure 2. The DOS and OPDOS diagrams for **1** and **2**.

and antibonding characteristics with respect to particular fragments. A positive value in OPDOS plots indicates a bonding interaction, while a negative value represents antibonding interaction and a value near zero indicates a non-bonding interaction. Additionally, the OPDOS diagrams allow the determination and comparison of the donor–acceptor properties of the ligands.

As can be seen from the OPDOS plots for **1** and **2**, N-heteroaromatic ligands have antibonding character in frontier HOMO molecular orbitals. In interactions of benzene with Ru(II), d orbitals have positive values in the energy range adequate to HOMO and HOMO-1, and in lower HOMO orbitals, the interaction has antibonding character. In the frontier occupied and virtual molecular orbitals, values of the interaction between ruthenium and 4,5-diphenylimidazole are small indicating the ligand as a weak π-acceptor. However, DMDIm is a stronger π-acceptor than 4,5-diphenylimidazole. For example, in HOMO, HOMO-1, and HOMO-2, ruthenium d orbitals participate in 38%, 36%, 35% and 2%, 2%, 3% 4,5-Ph_2Im in **2**. For **1**, in HOMO-5 and HOMO-7, the d_{Ru} levels are at 19% and 18%, respectively, and DMDIm at 26% and 52%. HOMO-4 is localized on the N-donor ligands (92%).

The energy decomposition analyses of **1** and **2** based on the work of Morokuma [13] and the extended transition state (ETS) partitioning scheme of Ziegler [14] have been carried out using ADF program (Release 2009.01) [15] at the level of B3LYP/TZP. The binding energy of the compound was calculated as the difference between the energy of complexes with the optimized geometry and the energies of the optimized ligands DMDIm or 4,5-Ph_2Im and fragment $[(C_6H_6)RuCl_{(2)}]$. General theoretical background on the bond energy decomposition scheme can be found in a review [16]. In table 4,

Table 4. Energy decomposition analysis for **1** and **2** in the $[(C_6H_6)RuCl_n]$ fragment and the DMDIm or 4,5-Ph_2Im ligands (energies in kcal mol^{-1}).

	$[(C_6H_6)RuCl(DMDIm)]^+$		$[(C_6H_6)RuCl_2(4,5\text{-}Ph_2Im)]$	
Energy [kcal mol^{-1}]	Gas phase	CH_3OH solvent	Gas phase	CH_3OH solvent
ΔE_{elstat}	−155.11	−157.86	−85.98	−85.98
$\Delta E_{kinetic}$	110.70	−148.32	28.23	129.02
$\Delta E_{Coulomb\ (Steric+OrbInt)}$	1.77	256.12	70.93	−1.11
ΔE_{XC}	−62.21	−40.34	−45.27	−64.99
$\Delta E_{solvation}$		−53.95		−31.53
ΔE	−104.86	−144.34	−32.08	−54.58

the results of energy decomposition analysis calculated for the complexes in gas phase and, more realistically, in methanol are listed. The Coulomb (steric and orbital interaction) energy plays an important role for $[(C_6H_6)RuCl]$ – DMDIm binding in solution and kinetic energy in **2**. The calculated bonding energies confirm the stronger π-accepting properties of DMDIm.

3.3. *Electronic spectra*

The UV-Vis spectra of the complexes display bands with maxima at 449.6 ($\log \varepsilon = 2.19$), 314.5 ($\log \varepsilon = 3.84$), 210.1 ($\log \varepsilon = 4.08$) nm – $[(C_6H_6)RuCl(DMDIm)]Cl$ and 412.6 ($\log \varepsilon = 3.70$), 283.2 ($\log \epsilon = 4.86$), 228.6 ($\log \varepsilon = 5.07$), 210.8 ($\log \varepsilon = 4.98$) nm – $[(C_6H_6)RuCl_2(4,5\text{-}Ph_2Im)]$. The experimental and calculated spectra of **1** are presented in figure 3. The longest wavelength experimental bands in **1** and **2** are assigned to transitions from HOMO, HOMO-1, and HOMO-2 to LUMO and LUMO + 1. As the molecular orbitals are mainly composed of the ruthenium d orbitals, the transitions are of *Ligand Field* type (d → d). The bands observed at 314.5 nm and 283.2 nm for **1** and **2**, respectively, have been attributed to *metal–ligand* and *ligand–metal charge transfer* transitions ($d \rightarrow \pi^*_{benzene/DMDIm/4,5\text{-}Ph2Im}$; $\pi^*_{DMDIm/Cl/4,5\text{-}Ph2Im} \rightarrow d$). In this energy region, the transitions between HOMO-3 → LUMO (62%), H–1 → LUMO + 2 (60%), HOMO-3 → LUMO + 2 (81%) for **1**, and HOMO → LUMO + 2 (89%), HOMO-1 → LUMO + 3 (43%), HOMO-4 → LUMO (80%), HOMO-4 → LUMO + 1 (61%) for **2** were calculated. The calculated transitions attributed to experimental ones at 210.1 nm (**1**) and 228.6 (shoulder), 210.8 nm (**2**) are *ligand–ligand charge transfer* type ($\pi \rightarrow \pi^*$).

4. Conclusion

In reactions between $[(C_6H_6)RuCl_2]_2$ and imidazole derivatives in methanol, two new half-sandwich ruthenium(II) complexes were obtained. In the reaction with 2,2′-bis(4,5-dimethylimidazolyl), $[(C_6H_6)RuCl(DMDIm)]Cl$ was synthesized, and with 4,5-diphenylimidazole, $[(C_6H_6)RuCl_2(4,5\text{-}Ph_2Im)]$. The molecular structures of the compounds were determined by X-ray and IR and ^{1}H-NMR results were studied. Based on the crystal structures, the electronic structures and UV-Vis spectra of the studied

Downloaded by [Renmin University of China] at 10:30 13 October 2013

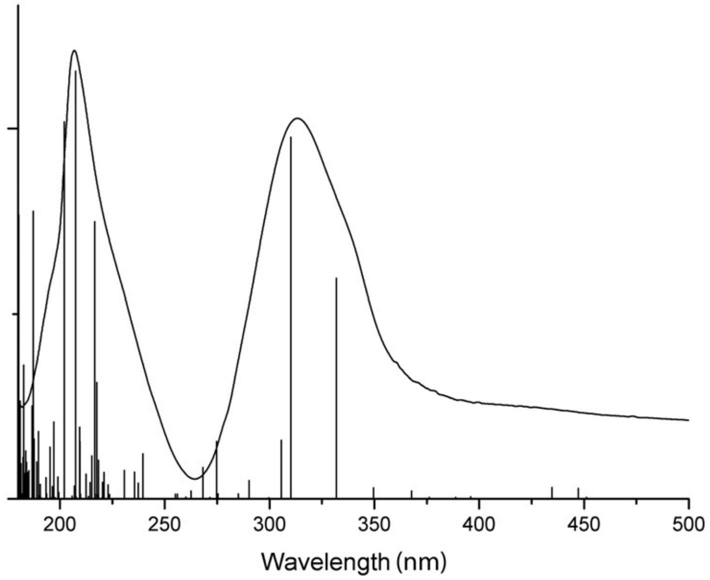

Figure 3. Experimental and calculated spectra of **1**.

compounds were calculated. The obtained results indicate that 2,2′-bis(4,5-dimethylimidazolyl) is a stronger π-acceptor than 4,5-diphenylimidazole. The electronic spectra of the complexes were calculated using the TD-DFT method. Analyses of the frontier orbitals of the complexes show contributions of ligands in visible region transitions.

Supplementary material

CCDC 755383 and CCDC 756607 contain the supplementary crystallographic data for the studied complexes. The data can be obtained free of charge from http://www.ccdc.cam.ac.uk/conts/retrieving.html, or from the Cambridge Crystallographic Data Centre, 12 Union Road, Cambridge CB2 1EZ, UK; Fax: +44-1223-336033; or E-mail: deposit@ccdc.cam.ac.uk. Calculations have been carried out in Wroclaw Centre for Networking and Supercomputing (http://www.wcss.wroc.pl).

References

[1] B. Therien. *Coord. Chem. Rev.*, **253**, 493 (2009); G. Pampaloni. *Coord. Chem. Rev.*, **254**, 402 (2010); L. Ronconi, J.P. Sadler. *Coord. Chem. Rev.*, **251**, 1633 (2007).

[2] I. de los Rios, M.J. Tenerio, M.A.J. Tenorio, M.C. Puerta, P. Valerga. *J. Organomet. Chem.*, **525**, 57 (1996); A. Schlüter, K. Bieber, W.S. Sheldrick. *Inorg. Chim. Acta*, **340**, 35 (2002); Y. Chen, M. Valentini, P.S. Pregosin, A. Albinati. *Inorg. Chim. Acta*, **327**, 4 (2002); A. Singh, N. Singh, D.S. Pandey. *J. Organomet. Chem.*, **642**, 48 (2002).

Downloaded by [Renmin University of China] at 10:30 13 October 2013

[3] C.S. Allardyce, P.J. Dyson, D.J. Ellis, S.L. Heath. *Chem. Commun.*, 1396 (2001); H. Chen, J.A. Parkinson, S. Parsons, R.A. Coxall, R.O. Gould, P.J. Sadler. *J. Am. Chem. Soc.*, **124**, 3064 (2002); R.E. Aird, J. Cummings, A.A. Ritchie, M. Muir, R.E. Morris, H. Chen, P.J. Sadler, D.I. Jodrell. *Br. J. Cancer*, **86**, 1652 (2002); R.E. Morris, R.E. Aird, P. Del, S. Murdoch, H. Chen, J. Cummings, N.D. Hughes, S. Parsons, A. Parkin, G. Boyd, D.I. Jodrell, P.J. Sadler. *J. Med. Chem.*, **44**, 3616 (2001).

[4] M.A. Bennett, T.-N. Huang, T.W. Matheson, A.K. Smith. *Inorg. Synth.*, **21**, 74 (1982).

[5] M.J. Frisch, G.W. Trucks, H.B. Schlegel, G.E. Scuseria, M.A. Robb, J.R. Cheeseman, G. Scalmani, V. Barone, B. Mennucci, G.A. Petersson, H. Nakatsuji, M. Caricato, X. Li, H.P. Hratchian, A.F. Izmaylov, J. Bloino, G. Zheng, J.L. Sonnenberg, M. Hada, M. Ehara, K. Toyota, R. Fukuda, J. Hasegawa, M. Ishida, T. Nakajima, Y. Honda, O. Kitao, H. Nakai, T. Vreven, J.A. Montgomery Jr, J.E. Peralta, F. Ogliaro, M. Bearpark, J.J. Heyd, E. Brothers, K.N. Kudin, V.N. Staroverov, R. Kobayashi, J. Normand, K. Raghavachari, A. Rendell, J.C. Burant, S.S. Iyengar, J. Tomasi, M. Cossi, N. Rega, J.M. Millam, M. Klene, J.E. Knox, J.B. Cross, V. Bakken, C. Adamo, J. Jaramillo, R. Gomperts, R.E. Stratmann, O. Yazyev, A.J. Austin, R. Cammi, C. Pomelli, J.W. Ochterski, R.L. Martin, K. Morokuma, V.G. Zakrzewski, G.A. Voth, P. Salvador, J.J. Dannenberg, S. Dapprich, A.D. Daniels, O. Farkas, J.B. Foresman, J.V. Ortiz, J. Cioslowski, D.J. Fox. *Gaussian 09, Revision A.1*, Gaussian, Inc., Wallingford CT (2009).

[6] A.D. Becke. *J. Chem. Phys.*, **98**, 5648 (1993); C. Lee, W. Yang, R.G. Parr. *Phys. Rev. B*, **37**, 785 (1988).

[7] M.E. Casida. In *Theoretical and Computational Chemistry*, J.M. Seminario (Ed.), Vol. 4, pp. 391–434, Elsevier, Amsterdam (1996).

[8] K. Eichkorn, F. Weigend, O. Treutler, R. Ahlrichs. *Theor. Chim. Acc.*, **97**, 119 (1997).

[9] N.M. O'Boyle, A.L. Tenderholt, K.M. Langner. *J. Comput. Chem.*, **29**, 839 (2008).

[10] O.V. Dolomanov, L.J. Bourhis, R.J. Gildea, J.A.K. Howard, H. Puschmann. *J. Appl. Cryst.*, **42**, 339 (2009).

[11] R. Tribo, J. Pons, R. Yanez, J.F. Piniella, A. Alvarez-Larena, J. Ros. *Inorg. Chem. Commun.*, **3**, 545 (2000); M. Jahncke, A. Neels, H. Stoeckli-Evans, G. Süss-Fink. *J. Organomet. Chem.*, **561**, 227 (1998); H. Kurosawa, H. Asano, Y. Miyaki. *Inorg. Chim. Acta*, **270**, 87 (1998).

[12] G.R. Desiraju, T. Steiner. *The Weak Hydrogen Bond in Structural Chemistry and Biology*, Oxford University Press, Oxford (1999); G.A. Jeffrey, W. Saenger. *Hydrogen Bonding in Biological Structures*, Springer-Verlag, Berlin (1994).

[13] K.J. Morokuma. *Chem. Phys.*, **55**, 1236 (1971).

[14] T. Ziegler, A. Rauk. *Theor. Chim. Acta*, **46**, 1 (1977).

[15] ADF2009.01, SCM, Theoretical chemistry, Vrije Universiteit, Amsterdam, The Netherlands. Available online at: http://www.scm.com

[16] F.M. Bickelhaupt, E.J. Baerends. In *Reviews in Computational Chemistry*, K.B. Lipkowitz, D.B. Boyd (Eds), Vol. 15, pp. 1–86, Wiley-VCH, New York (2000).

Downloaded by [Renmin University of China] at 10:30 13 October 2013